 SDHM, vol.9, no.1, pp.21-41, 2013

# Damage Propagation in Composite Structures using an Embedded Global-Local Approach

**A. Riccio[1], M. Zarrelli[2] and F. Caputo[1]**

**Abstract:** In the present paper a three-dimensional Progressive Damage Approach (PDA) for laminated composites will be presented. This approach is based on the use of a progressive damage finite element with the geometrically non-linear finite element formulation for stress calculation. The FEM element has been integrated with Hashin's failure criteria to split fibre and matrix failure modes and to simulate stiffness degradation within each ply by means of the Ply Discount Method (PDM). FEM code previsions, in the case of complex structures with different mesh densities and element types, were compared with the results obtained using embedded global-local approach to prove the effectiveness of the implemented code. As experimental test-case, the structural behaviour of a notched panel, under tensile load has been investigated. Obtained numerical results have been compared with both numerical and experimental data, available from the literature. Finally, a comparison between a full 3D model and a global-local model has been performed in order to evaluate the effectiveness of the developed progressive damage approach in global-local analyses..

**Keywords:** progressive damage, failure criteria, degradation rules, global-local approach.

## 1 Introduction

Composite materials are commonly used in aircraft structures. The strength, the stiffness and the lightweight properties of composites make their use very attractive, but the brittle failure, characterising their structural behaviour, is a real obstacle to the development of a fully composite oriented design philosophy. Hence a deep understanding of their strength and failure modes is very important in order to provide reliable design of composite structures. For example, laminated composite structures can develop local failure or exhibit local damage such as matrix

[1] The Second University of Naples - DIAM, Aversa (CE), Italy.
[2] CNR-Research National Council - IMCB, Portici (NA), Italy.

cracks, fibre breakage, fibre-matrix de-bonds, and delaminations under normal operating conditions which may contribute to their failure. The ability to predict the initiation and growth of such damage is essential for predicting the performance of composite structures and developing reliable, safe designs that exploit the advantages offered by composite materials.

In recent years, the progression of damage in composite laminates has focused an extensive research work. Ochoa and Reddy (1992) and Sleight (1999), Sleight et al. (1997) presented an excellent overview of the basic steps in performing a progressive failure analysis. These basic steps have been investigated and commented in Tessler and Riggs (1994) underlining the complexity of this type of analysis based on five different key features. The first is a non-linear analysis capability used to establish the equilibrium; the second, an accurate stress recovery procedure is needed in order to evaluate the local lamina stress-state; the third, is a failure criterion required to detect local lamina failure and to determine the mode of failure; the fourth, is a material degradation or damage model to estimate local material properties during the delamination propagation; finally, the fifth, is a procedure to re-establish the equilibrium state being altered the local lamina properties. Initial failure of a layer within a laminate of a composite structure can be predicted by applying an appropriate failure criterion or first-ply failure theory. Various failure criteria have been proposed in literature [Paris (2001); Nahas (1986); Armentani et al. (2004); Tsai (1984); Reddy and Pandey (1987); Tsai and Wu (1971); Hashin (1980); Hashin and Rotem (1973); Caputo et al. (2006); Sandhu (1974)]. Most failure criteria are based on the stress-state in a lamina. Ideally, a 3D-dimensional model is desirable for obtaining accurate stresses and strains. However, due to the extensive amount of computational time required for a three-dimensional analysis, two-dimensional models can be adopted too. Among the several failure criteria, Hashin (1980); Hashin and Rotem (1973) proposed a quadratic failure criterion in piecewise form on material strengths, where each smooth branch represents a failure mode. When a material allowable value of failure criteria is exceeded in a given layer, the engineering material constants corresponding to the particular mode of failure are reduced according to the material degradation model. A number of post-failure material property degradation models have been proposed for progressive failure analysis. Most of these material degradation models belong to one of three general categories: instantaneous unloading [Murray and Schwer (1990)], gradual unloading Chang and Chang (1987); Petit and Waddoups (1969) and constant stress at ply failure [Hahn and Tsai (1983)]. One of the most common methods used for degradation of material properties is the ply-discount theory [Murray and Schwer (1990)], which belongs to the instantaneous unloading category. In the past two decades, some researchers have given examples of progressive damage approaches Reddy and Pandey (1987); Pandey and Reddy (1987); Tolson and Zabaras (1991); Coats (1996); Lo et al. (1996); Coats and Harris (1998); Reddy and Reddy (1993).

In Reddy and Pandey (1987), a finite element procedure based on first-order shear deformation theory for first-ply failure analysis of laminated composite plates is presented. The method based on Tsai-Hill, Tsai-Wu and Hoffman failure criteria worked very well for in plane-loading conditions but it reports inconsistency in simulating progressive failure when transverse loading conditions were applied. In Pandey and Reddy (1987), a linear analysis approach is adopted to predict the behaviour of a laminated plate with hole subjected to uniaxial tension. However, no comparison with experimental results is provided.

In Coats (1996); Lo et al. (1996); Coats and Harris (1998), Coats developed a non-linear progressive failure analysis for laminated composites that used a constitutive model describing the kinematics of matrix cracks via volume averaged internal state variables. The evolution of the internal state variables was governed by an experimentally based damage evolutionary relationship. The methodology was used to predict the initiation and growth of matrix cracks and fibre fracture. Most of the residual strength predictions were within 10% of the experimental failure loads.

In the present paper the modular three-dimensional progressive damage approach for laminated composites implemented in ANSYS [ANSYS (1994)] and tested in Riccio and Marciano (2005); Riccio (2005), has been used to develop a progressive damage finite element based on the geometrically non-linear finite element formulation for stress and strain calculation, in the commercial FEM code B2000 [SMR (2005)]. The FEM element has been integrated with Hashin's failure criteria to split fibre and matrix failure modes and with the ply discount method to simulate the stiffness degradation in each ply. The FEM tool was tested together with an embedded global-local approach (based on the interface technology) in order to prove its effectiveness when dealing with complex structures that need to be modelled by using different mesh densities and different element types. In the next sections the theoretical basis of the implemented progressive damage procedure is briefly introduced and the results of numerical analyses are shown. As an application, the structural behaviour of a notched panel under tensile load has been investigated and the numerical results obtained have been compared with literature numerical and experimental data [Coats and Harris (1998)]. Finally, a comparison between a full 3D model and a global-local model has been performed in order to evaluate the effectiveness of the adopted progressive damage approach in conjunction with an embedded global-local approach.

## 2 Theoretical Background

In this section, the theoretical background of the proposed progressive damage approach will be introduced. The stress evaluation, the failure criteria application and the material properties degradation rules are components of the suggested formulation that need to be considered simultaneously for the simulation of the functional behaviour of composite structures with damage on-set and propagation. These components will be briefly described below.

### *2.1 Stress evaluation*

For stress evaluation, large displacements and large rotations (geometrical nonlinearity) have been taken into account by means of the Green Lagrange strain tensor that, for the Total Lagrangian Formulation, can be written:

$$ {}^{t+\Delta t}_{0}e_{ij} = {}^{t}_{0}e_{ij} + {}_{0}\varepsilon_{ij} \tag{1} $$

$$ {}_{0}\varepsilon_{ij} = {}_{0}e_{ij} + {}_{0}\eta_{ij} \tag{2} $$

with

$$ {}_{0}e_{ij} = \frac{1}{2}\left({}_{0}u_{i,j} + {}_{0}u_{j,i} + {}^{t}_{0}u_{k,i} \cdot {}_{0}u_{k,j} + {}_{0}u_{k,i} \cdot {}^{t}_{0}u_{k,i}\right) \tag{3} $$

$$ {}_{0}\eta_{ij} = \frac{1}{2}\left({}_{0}u_{k,i} \cdot {}_{0}u_{k,j}\right) \tag{4} $$

where ${}_{0}e_{ij}$ and ${}_{0}\eta_{ij}$ are, respectively, the linear and non linear part of strain tensor and ${}_{0}u_{i,j} = \frac{\partial u_i}{\partial^0 x_j}$. The subscript 0 states that the quantities are calculated with reference to the time 0. The stresses are represented by means of the second Piola-Kirchhoff tensor that can be written:

$$ {}^{t+\Delta t}_{0}S_{ij} = {}^{t}_{0}S_{ij} + {}_{0}S_{ij} \tag{5} $$

In order to apply the failure criteria, the Cauchy Stresses are needed, that can be calculated using the relation:

$$ t_{\tau} = \frac{{}^{t}\rho}{{}^{0}\rho} {}^{t}_{0}X \cdot {}^{t}_{0}S_{ij} \cdot {}^{t}_{0}X^{T} \tag{6} $$

where $t_{\tau}$ is the Cauchy Stresses tensor and ${}^{t}_{0}X$ is the deformation gradient at time $t$.

### *2.2 Failure criteria application*

From the Cauchy Stress distribution, by means of suitable failure criteria, it is possible to predict the location and the type of damage. In the present FEM model the Hashin's failure criteria have been adopted since they can separately predict the fibre breakage and the matrix cracking of each layer. In fact, in the Hashin's formulation is characterised by distinct polynomials associated to the different failure modes. In our three-dimensional problem, we have considered the following failure modes :

Matrix tensile failure ($\sigma_{yy} > 0$);

$$\left(\frac{\sigma_{yy}}{Y_t}\right)^2 + \left(\frac{\sigma_{xy}}{S_{xy}}\right)^2 + \left(\frac{\sigma_{yz}}{S_{yz}}\right)^2 \geq 1 \tag{7}$$

Matrix compression failure ($\sigma_{yy} < 0$);

$$\left(\frac{\sigma_{xx}}{Y_t}\right)^2 + \left(\frac{\sigma_{xy}}{S_{xy}}\right)^2 + \left(\frac{\sigma_{xz}}{S_{yz}}\right)^2 \geq 1 \tag{8}$$

Fibre tensile failure ($\sigma_{xx} > 0$);

$$\left(\frac{\sigma_{xx}}{X_t}\right)^2 + \left(\frac{\sigma_{xy}}{S_{xy}}\right)^2 + \left(\frac{\sigma_{xz}}{S_{xz}}\right)^2 \geq 1 \tag{9}$$

Fibre compression failure ($\sigma_{xx} < 0$);

$$\left(\frac{\sigma_{xx}}{X_c}\right) \geq 1 \tag{10}$$

Fibre-matrix shear-out failure ($\sigma_{xx} < 0$);

$$\left(\frac{\sigma_{xx}}{X_c}\right)^2 + \left(\frac{\sigma_{xy}}{S_{xy}}\right)^2 + \left(\frac{\sigma_{xz}}{S_{xz}}\right)^2 \geq 1 \tag{11}$$

Fibre-Kinking failure ($\sigma_{xx} < 0$);

$$\left(\frac{\sigma_{xx}}{X_c}\right)^2 + \left(\frac{\sigma_{xz}}{S_{xz}}\right)^2 \geq 1 \tag{12}$$

In the above equations, $\sigma_{ij}$are the stress components in the $ij$ direction and $S_{ij}$, $Y_t$, $X_t$, $Y_c$, $X_c$, are the material strengths.

### 2.3 Material property degradation rules

The material property degradation rules are applied to account for the post-damage material behaviour of each layer. This is necessary in order to perform a progressive failure analysis until global failure. For each of the failure modes above mentioned, according to the ply discount approach [Murray and Schwer (1990)], an appropriate property degradation rule has been introduced according to the physics of the damage mechanisms.

Matrix tensile and compression failure;

$$\begin{aligned} &\bar{E}_y = k \cdot E_y \\ &\bar{E}_z = k \cdot E_z \\ &\bar{G}_{yz} = k \cdot G_{yz} \end{aligned} \tag{13}$$

Fibre tensile and compression failure;

$$\begin{aligned} &\bar{E}_x = k \cdot E_x \\ &\bar{G}_{xy} = G_{yz} \\ &\bar{G}_{xz} = G_{yz} \end{aligned} \tag{14}$$

Fibre-matrix shear-out failure;

$$\begin{aligned} &\bar{G}_{xy} = G_{yz} \\ &\bar{G}_{xz} = G_{yz} \end{aligned} \tag{15}$$

Fibre-Kinking failure;

$$\begin{aligned} &\bar{E}_x = k \cdot E_x \\ &\bar{E}_y = k \cdot E_y \\ &\bar{E}_z = k \cdot E_z \\ &\bar{G}_{xy} = k \cdot G_{yz} \\ &\bar{G}_{xz} = k \cdot G_{yz} \\ &\bar{G}_{yz} = k \cdot G_{yz} \end{aligned} \tag{16}$$

where $k$ is a degradation factor and the over-lined properties indicate the corresponding degraded values. Regardless of its physical meaning, in the present work the degradation factor, k, is introduced to avoid convergence problems and to speed-up the progressive damage procedure. In order to have an instantaneous degradation rule, the ideal case would be the case of $k = 0$ but performed simulation with presented numerical model shows that a practical value of $k = 0.1$ is found to work very well. By using this value for the $k$ parameter, the material properties are degraded enough so that they can be considered negligible, while, at the same time, the simulation is kept stable sufficiently to reach the convergence at each step. To avoid excessive element distortions and Jacobian singularity when failure in all plies occurs, the material properties for completely failed elements are increased in the normal contact direction in order to make the element incompressible under contact pressure.

## 3 Numerical Procedure

The numerical code chosen for the implementations is the "research-oriented" finite element software, B2000. This code is characterised by a modular structure with processors exchanging data through a database called MEMCOM. In order to implement the progressive damage procedure in B2000, some modules have been created and some others have been modified. The new and the modified modules of B2000 are represented in the schematic view of B2000 structure shown in figure 1.

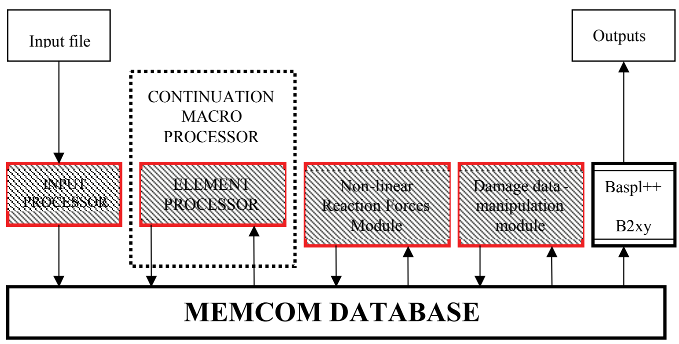


Figure 1: Schematic Representation of the B2000 structure with PDA approach.

The input and the element processors have been modified in order to read the progressive damage input variables and to update the material matrix during the progressive damage analysis. A new module for the calculation of reaction forces in non-linear analyses with applied displacements and new module for the manipulation of data coming from the non-linear progressive damage analyses have been implemented. The PDA module is necessary due to the large amount of information coming from PDA analyses and describing the damage status for each ply within the single element at each cycle. In figure 2 the flow chart, representing the progressive damage procedure implemented in B2000, is shown.

The Procedure can be summarised as follows. Firstly, geometry, material layout and properties, boundary conditions and initial loads are defined and read by the input processor. Then in the progressive damage element, the calculation of stiffness matrix, forces vector and Cauchy Stresses (transformation from $2^{nd}$ Piola Kirchhoff Stresses to Cauchy Stresses) is performed. At the beginning of a new time step (cycle) failure check is carried out. If necessary, then, the material properties are degraded at ply level. The convergence and the iteration number are checked inside the continuation macro-processor; if convergence is achieved, then the load is increased and the procedure can be repeated, otherwise, the structure is supposed to be completely failed.

After the calculations, the non-linear reaction forces module is used to calculate the reaction forces at each step for analyses with applied displacements. The damage data-manipulation modules is then used to create data-sets in MEMCOM containing all the useful output quantities describing the damage status in each ply of each element at each step. These data-sets, as mentioned above, are structured in such a way to be readable by the B2000 visual module. The use of this approach makes possible to monitor the progressive failure of composites in each ply of each element during the loading process.

## 4 Notched Panel by Progressive Damage Approach (PDA): code validation

### *4.1 Geometry, materials, FEM mesh, boundary conditions and applied loads*

For validation purpose of the implemented FEM approach, experimental results of typical testing campaign on centre-notched tensile specimens, reported by Coats and Harris (1998), were considered. The geometrical dimensions and the properties of the laminae used, are presented in Figure 3. The stacking sequence of the composite notched panel was $\left(\mp 45/0/09/\mp 30/\bar{0}\right)_S$; moreover, holding plane symmetry conditions only a quarter of the panel has been analysed. Two B2000 models have been created: a full 3D model and a 3D-2D model. In the figure 4 a schematic representation of the two analysed models is presented.

The B2000 FEM models have been divided into four branches, as shown in figure 4. The layered brick elements have been used for the 3-dimensional part of the models while the orthotropic plate elements have been used for the 2-dimensional part of the model. For the connection between the 2D and 3D part the embedded global-local method implemented in the B2000 has been adopted. In the first two branches (branch 1 and branch 2) the progressive failure elements have been used while in the other two branches (branch 3 and branch 4) the ordinary layered brick elements have been used in order to optimise the dimension of database files and the computational time. Two different mesh densities were adopted aiming to investigate the influence of discretization on the convergence of the results.

The different meshes are shown in figure 5. A single element with 13 layers, whose

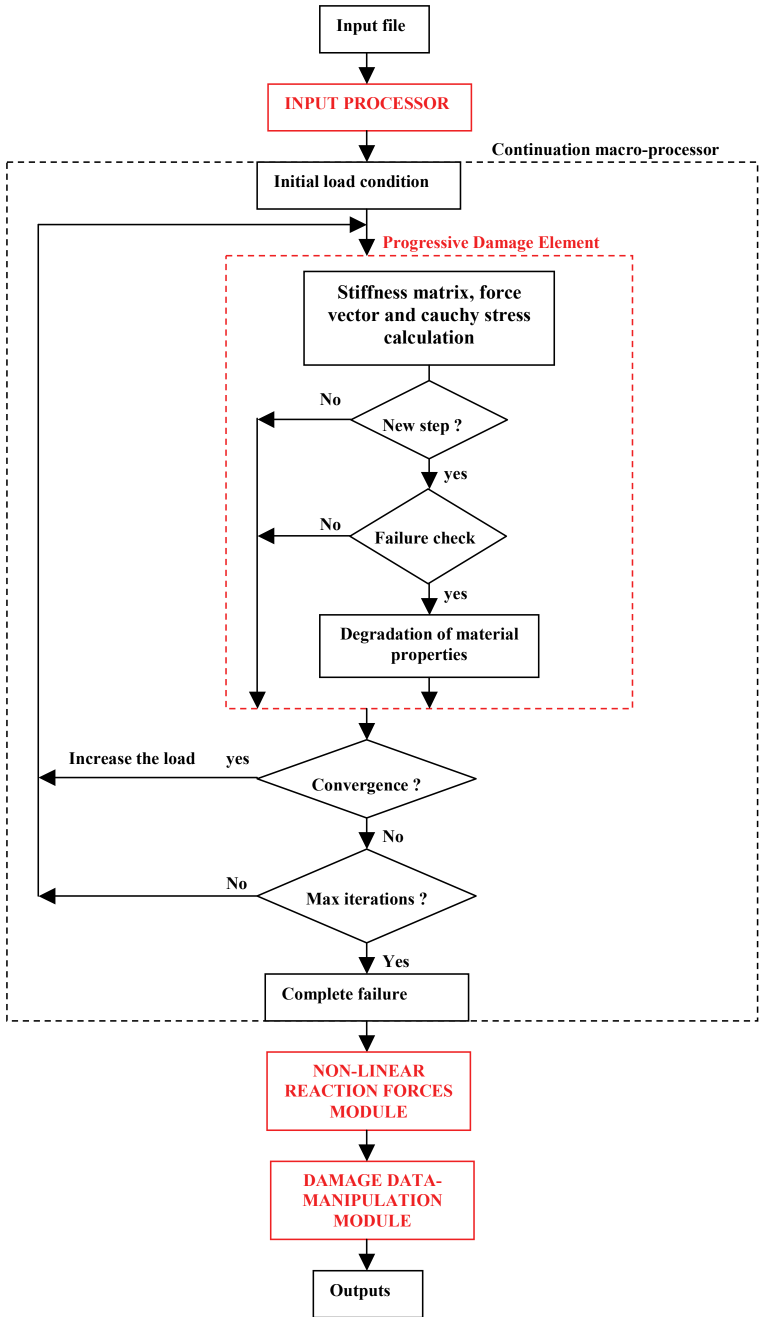


Figure 2: Chart of the progressive damage approach implemented in B2000.

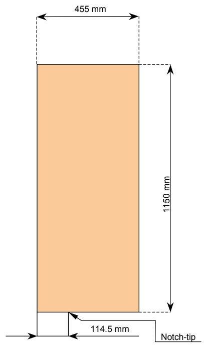


| | Property | AS4/938 |
|---|---|---|
| Ply longitudinal modulus | $E_1$ | 135.1 GPa |
| Ply transverse modulus | $E_2$ | 9.38 GPa |
| Ply transverse modulus | $E_3$ | 9.38 GPa |
| In-plane shear modulus | $G_{12}$ | 4.96 GPa |
| Out-of-plane shear modulus | $G_{13}$ | 4.96 GPa |
| Out-of-plane shear modulus | $G_{23}$ | 4.96 GPa |
| Poisson's ratio | $\nu_{12}$ | 0.032 |
| Poisson's ratio | $\nu_{13}$ | 0.032 |
| Poisson's ratio | $\nu_{23}$ | 0.51 |
| Maximum ply tensile stress at 0° | $\sigma_{1t}$ | 2280 Mpa |
| Maximum ply tensile stress at 90° | $\sigma_{2t}$ | 57 Mpa |
| Maximum out-of-plane ply tensile stress | $\sigma_{3t}$ | 57 Mpa |
| Maximum ply compressive stress at 0° | $\sigma_{1c}$ | 1440 Mpa |
| Maximum ply compressive stress at 90° | $\sigma_{2c}$ | 228 Mpa |
| Maximum ply out-of-plane compressive stress | $\sigma_{3c}$ | 228 Mpa |
| Maximum ply in-plane shear stress | $\sigma_{12}=\sigma_{13}$ | 71 Mpa |
| Maximum ply out-of-plane shear stress | $\sigma_{23}$ | 71 Mpa |

Figure 3: notched panel Geometry and material properties.

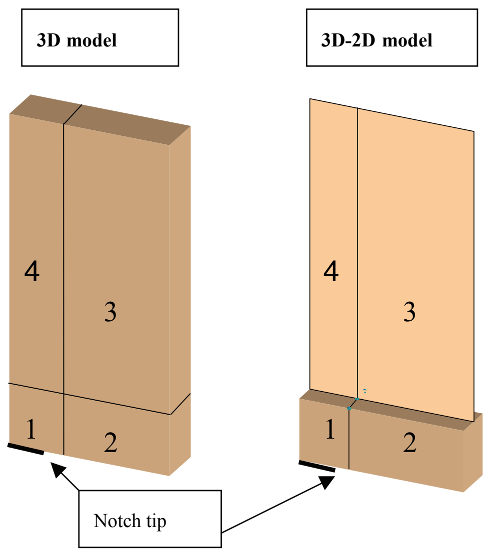


Figure 4: Schematic Representation of the two models.

orientation is shown in fig. 6, has been placed along the thickness.

The boundary conditions applied to our models are schematically shown in the figure 7. As above mentioned, a quarter of the panel has been considered in our computations due to the symmetry with respect to the two axes of the laminate plane. The panel has been loaded by means of applied displacements.

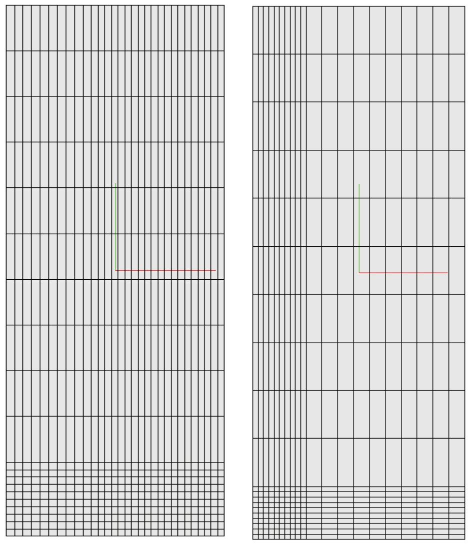

Figure 5: FEM meshes used for the notched panel.

| Element | layer | Orientation |
|---|---|---|
| ELEMENT 1 | 13 | -45 |
| | 12 | 45 |
| | 11 | 0 |
| | 10 | 90 |
| | 9 | +30 |
| | 8 | -30 |
| | 7 | 0 |
| | 6 | -30 |
| | 5 | +30 |
| | 4 | 90 |
| | 3 | 0 |
| | 2 | 45 |
| | 1 | -45 |

Figure 6: Stacking sequence in the composite panel.

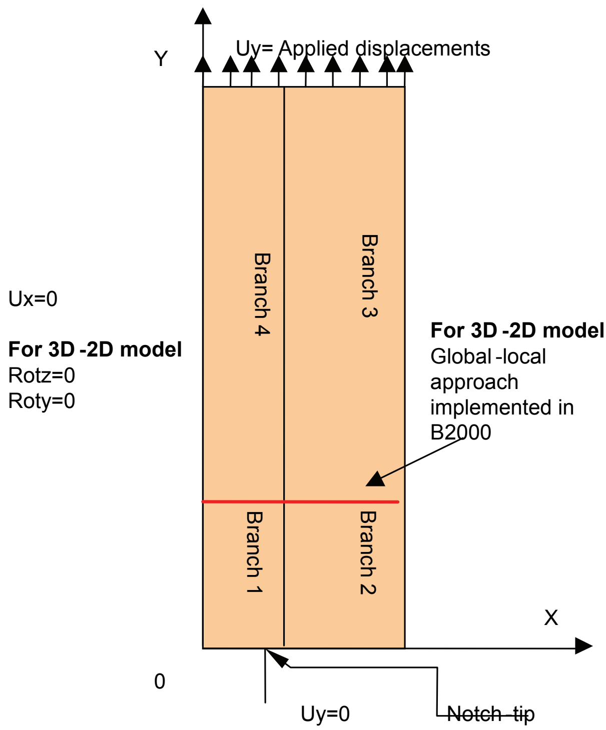


Figure 7: Boundary conditions and applied load.

### 4.2 *Numerical Results*

The obtained numerical results for the full 3D model of the notched panel have been evaluated and compared with experimental and numerical data from Coats and Harris (1998) in order to check the effectiveness of the proposed numerical progressive damage procedure. In figure 8 the comparison between numerical results in terms of load vs. displacement curves obtained for the two different adopted meshes are presented. The mesh can influence the first ply failure load, leading to an overestimated final failure load, mainly due to the singularity of the stresses near the notch tip. The experimental value of the final failure load reported in Coats and Harris (1998) is 165 kN. The overestimation of our numerical model can be due to the lack of control, on the time step, when the failure is found. Actually, in our implementations the size of time step is not dependent on the check for failure; this fact cannot guarantee the correct redistribution of the stresses in the elements after failure. Furthermore, the lack of PDA elements in branch 3 and branch 4 can also influence the quality of results. In figure 9 the Y-displacement distribution on the deformed shape of the notched panel is shown with an amplification factor of 20.

The numerical results in terms of damage propagation at the 88% of the final failure load, obtained by the present model, have been compared with the results reported by Coats and Harris (1998); comparisons are made for all the differently oriented plies of the notched panel in the figs 11-22, respectively for –45°, +45°, 0°, 90°,+30° and -30° plies. In order to understand the B2000 outputs, table 2 associates the failure mode detected in the ply to the numbers shown by baspl++. In figure 10 the numerical results in terms of damage propagation in the different plies of the notched panel found with the model proposed in Coats and Harris (1998) are presented.

Some interesting observation can be made about the results shown in the previous figures. Matrix and fibre failures have been found near the notch tip for +45°, -45° oriented plies; while shear-out and matrix failures have been found near the notch tip for +30° and –30° oriented plies. 90° oriented plies undergo shear-out failure mechanism together with a wide region of matrix failure; while, 0° oriented plies report no failure under the loading conditions assumed for this procedure validation. From the comparison between figure 10 and figures 11-16, the good agreement between the progression of damage computed by the two different approaches can be pointed out.

However, by the B2000 model, the extended fibre fracture along the x-axis direction for the 0°-oriented ply has not been picked up. This is in agreement with the experimental results shown in Coats and Harris (1998), where the fibre fracture extension along the x direction was only relative to a reduced portion of fiber discretization of a length of about 5 mm.

### *4.3 Numerical Results*

In order to test the effectiveness of the proposed progressive damage approach in global-local analyses, the 3D-2D model of the notched panel, above described, has been used for calculations. In figure 17 the comparison between 3D-2D model numerical results in terms of load-displacement curve obtained for the two different adopted meshes is presented. As previously seen for the full 3D model, the mesh can influence the first ply failure load, leading to an over-estimated final failure load. In order to evaluate the approximations introduced using 2D elements, a comparison between the full 3D model and the 3D-2D model in terms of load-displacement curves is presented in figure 18.

As it can be noted in figure 18, the use of 2D elements instead of 3D elements in the branch 3 and branch 4 of the model does not alter the tensile behaviour in terms of load-displacement curves. In particular, the first ply failure loads and the final

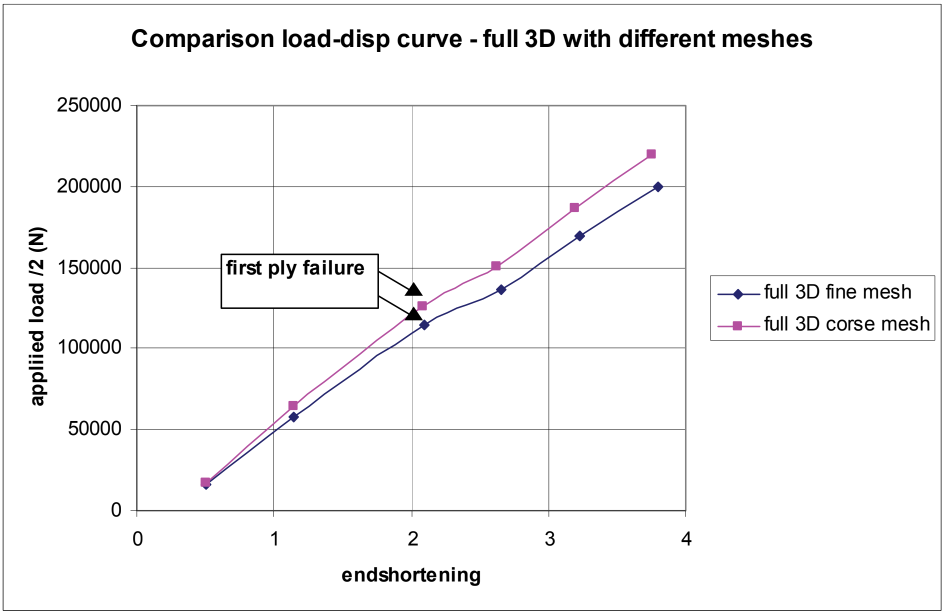


Figure 8: Full 3D model - Applied tensile load versus end-shortening: comparison between two mesh sizes.

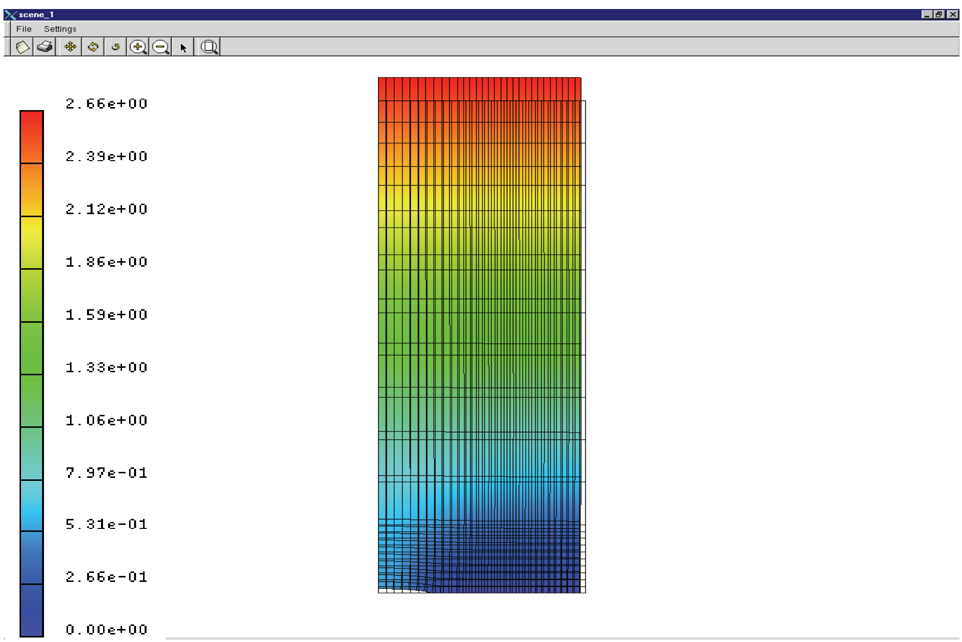


Figure 9: Deformed shape (ampl. 20) – distribution of Y displacements.

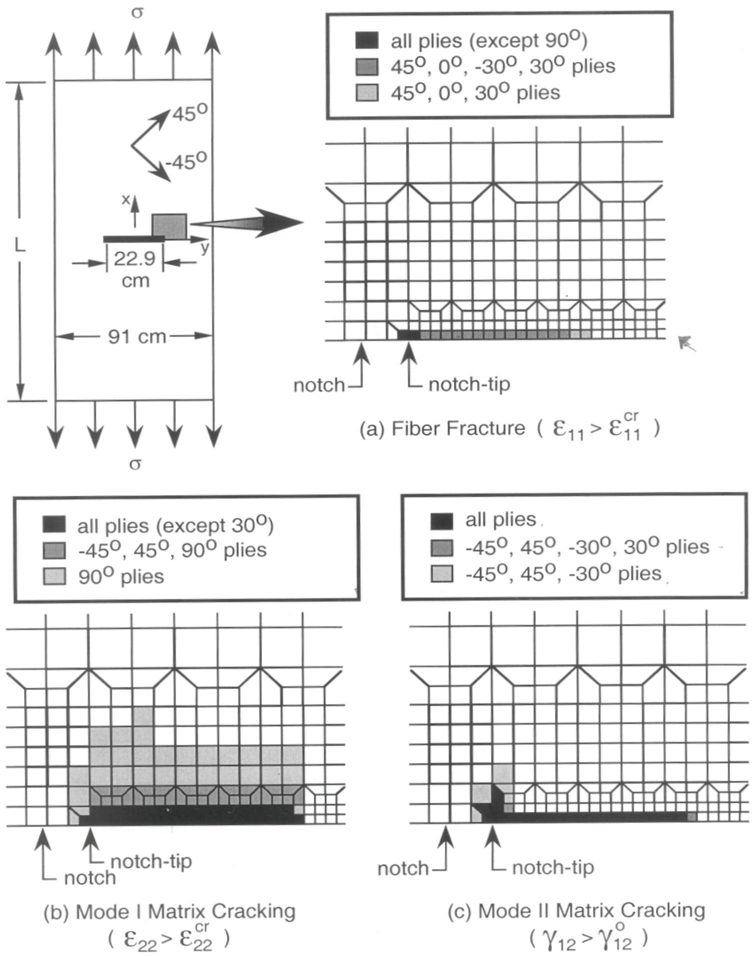


Figure 10: Numerical progression of damage in the plies of the notched panel presented in [Tessler and Riggs (1994)].

failure loads are almost identical for the two models.

In order to quantify the differences between the full 3D model and the 3D-2D model in terms of damage progression, in figure 19-24 the numerical results in terms of damage propagation respectively in the –45, +45, 0, 90,+30 and -30 plies of the notched panel, found with the present 3D-2D model at the 88% of the final failure load, are presented.

The results shown in the previous figures are almost identical to the ones obtained with the full 3D model. The small differences for the 90° oriented plies are due

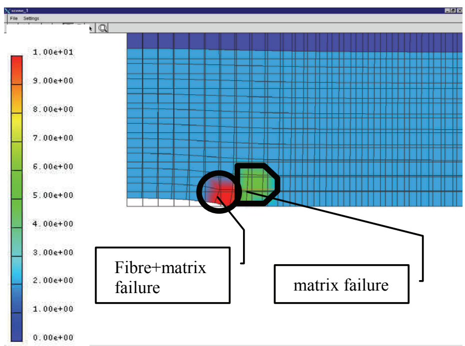


Figure 11: Numerical progression of damage in the -45° plies of the notched panel – full 3D model

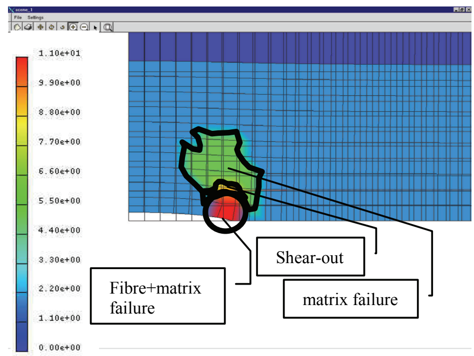


Figure 12: Numerical progression of damage in the 45° plies of the notched panel full 3D model

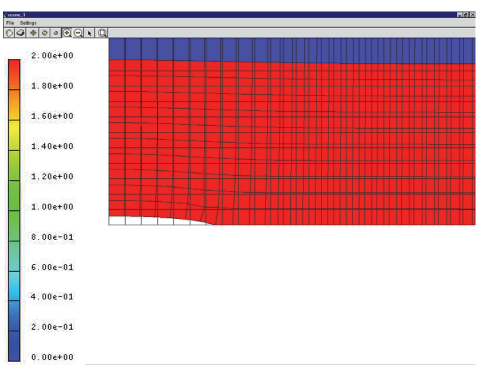


Figure 13: Numerical progression of damage in the 0° plies of the notched panel – full 3D model

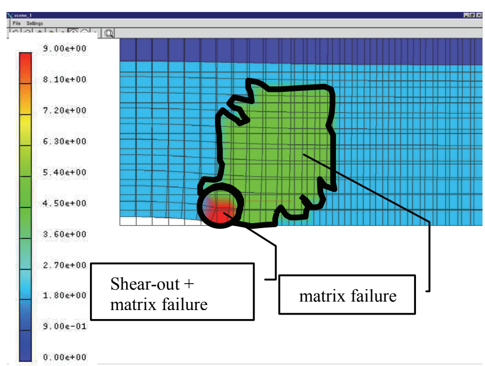


Figure 14: Numerical progression of damage in the 90° plies of the notched panel – full 3D model

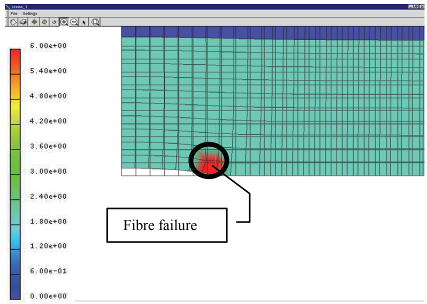


Figure 15: Numerical progression of damage in the 30° plies of the notched panel – full 3D model of the notched panel – full 3D model

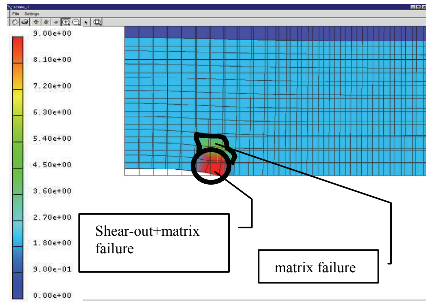


Figure 16: Numerical progression of damage in the -30° plies of the notched panel – full 3D model

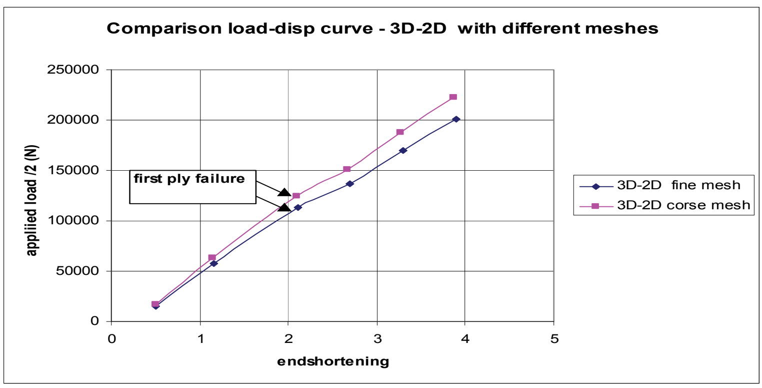


Figure 17: 3D-2D model - Applied tensile load versus end-shortening: comparison between two mesh sizes.

essentially to the slight difference in the load levels at the examined steps. From the point of view of the damage progression small difference in the level of load can cause relevant variations in the number of "broken" elements, especially for matrix failure.

## 5 Conclusions

A three-dimensional progressive damage approach for Finite Element analyses has been presented. The proposed methodology, based on the Hashin's failure criteria and sudden material properties degradation rules, has proved to be able to follow

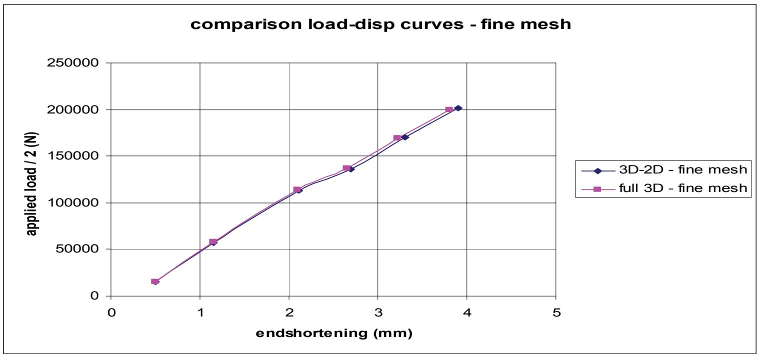


Figure 18: Applied tensile load vs end-shortening: comparison between full 3D model and 3D-2D model.

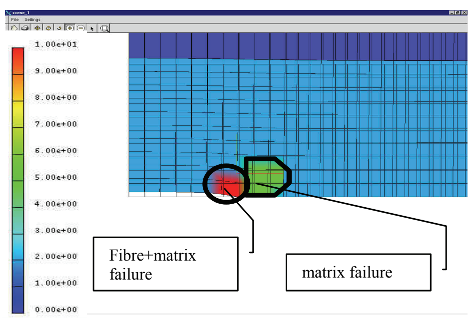


Figure 19: Numerical progression of damage in the –45° plies of the notched panel – 3D-2D model

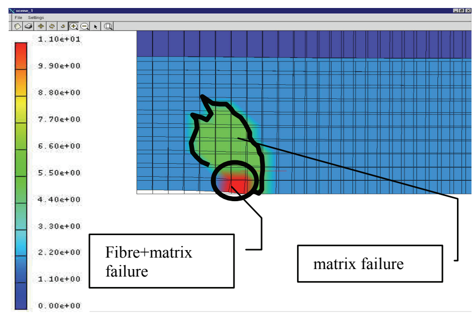


Figure 20: Numerical progression of damage in the 45° plies of the notched panel – 3D-2D model

the damage progression at ply level in composite structures. Using the experimental and numerical results of a simple notched composite panel available in literature, the proposed approach has been validated.

First, non-linear analyses on a complete 3D model have been carried out in order to evaluate the effectiveness of the implemented methodologies. The influence of mesh has been briefly investigated. The agreement between the literature experimental/numerical results and the predictions obtained by the present model is very good. The same-notched panel has been modelled considering 3D and 2D elements joined by means of an embedded global-local technique. The two different models have been compared in terms of load-displacement curves and damage progression for each ply, giving almost identical results.

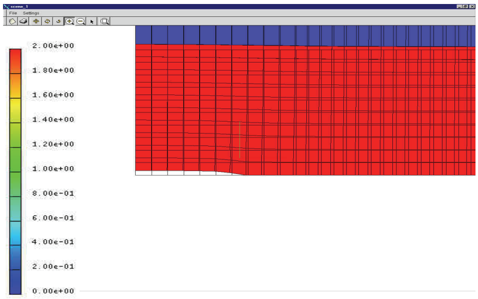

Figure 21: Numerical progression of damage in the 0° plies of the notched panel – 3D-2D model

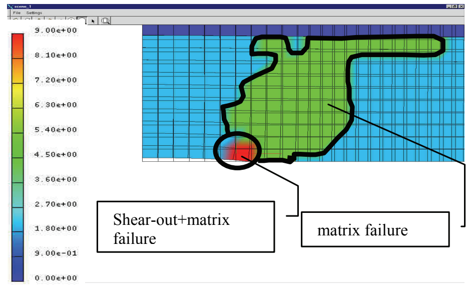


Figure 22: Numerical progression of damage in the 90° plies of the notched panel – 3D-2D model

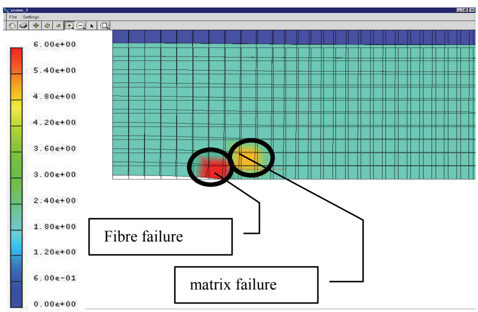


Figure 23: Numerical progression of damage in the 30° plies of the notched panel – 3D-2D model

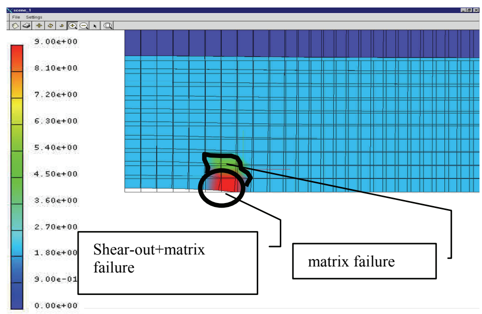


Figure 24: Numerical progression of damage in the -30° plies of the notched panel – 3D-2D model

However, some modifications could be made in order to better fit the reference results: control of time step dependent on check for failure in the elements, implementation of delamination on-set and growth criteria and the control of the degradation factor $k$ according to more realistic and less empiric degradation rules.

## References

**ANSYS, Inc.** (1994): ANSYS MANUALS (release 5.3). Houston US.

**Armentani, E., Caputo, F., Esposito, R., Godono, G.** (2004): Evaluation of energy release rate for delamination defects at the skin/stringer interface of a stiffened composite panel, *Engineering Fracture Mechanics*, Vol. 71/4-6, pp 885-895.

**Caputo, F., Lamanna, G., Soprano, A.** (2006): Numerical Investigation on the Crack Propagation in a Flat Stiffened Panel, *Key Engineering Materials*, vols. 324-325, pp. 559-562.

**Chang, F. K., Chang, K. Y.** (1987): A Progressive Damage Model for Laminated Composites Containing Stress Concentrations, *Journal of Composite Materials*, Vol. 21, pp. 834-855.

**Coats, T. W.** (1996): A Progressive Damage Methodology for residual Strength Predictions of Center-Crack Tension Composite Panels, Ph. D. Dissertation, Old Dominion University.

**Coats, T. W., Harris, C. E.** (1998): A Progressive Damage Methodology for residual Strength Prediction of Notched Composite Panels, NASA TM-1998-207646.

**Hashin, Z.** (1980): Failure Criteria for Unidirectional Fiber Composites, ASME Journal of Applied Mechanics, Vol. 47, pp. 329-334.

**Hahn, H. T., Tsai, S. W.** (1983): On the Behavior of Composite Laminates After Initial Failure, *Astronautics and Aeronautics*, Vol. 21, pp. 58-62.

**Hashin, Z., Rotem, A.** (1973): A Fatigue Failure Criterion for Fiber Reinforced Materials, *Journal of Composite Materials*, Vol. 7, pp. 448-464.

**Lo, D. C., Coats. T. W., Harris, C. E., Allen, D. H.** (1996): Progressive Damage Analysis of Laminated Composite (PDALC) (A computational Model Implemented in the NASA COMET Finite Element Code, NASA TM 4724.

**Murray, Y., Schwer, L.** (1990): Implementation and Verification of Fiber-Composite Damage Models, Failure Criteria and Analysis in Dynamic Response, *ASME AMD*, Vol. 107, pp. 21-30.

**Nahas, M. N.** (1986): Survey of Failure and Post-Failure Theories of Laminated Fiber-Reinforced Composites, *Journal of Composites Technology and Research*, Vol. 8, No. 4, pp. 138-153.

**Ochoa, O., Reddy, J. N.** (1992): Finite Element Analysis of Composite Laminates, Kluwer Academic Publishers, Dordrecht, The Netherlands.

**Pandey, A. K., Reddy, J. N.** (1987): A Post First Ply Failure Analysis of Composite Laminates, AIAA Paper 87-0898, Proceedings of the AIAA/ASME/ASCE/AHS/ASC 28th Structures, Struct. Dyn. Mat. Conf., pp. 788-797.

**Paris, F.** (2001): A Study of Failure Criteria of Fibrous composite Materials, NASA/CR-2001-210661.

**Petit, P. H., Waddoups, M. E.** (1969): A Method of Predicting the Nonlinear Behavior of Laminated Composites, *Journal of Composite Materials*, Vol. 3, pp. 2-19.

**Reddy , Y. S., Reddy, J. N.** (1993): Three-dimensional Finite Element Progressive Failure Analysis of Composite Laminates Under Axial Extension, *Journal of Composite Technology and Research*, V.15, N.2, pp. 73-87.

**Reddy, J. N., Pandey, A. K.** (1987): A First-Ply Failure Analysis of Composite Laminates, *Computers and Structures*, Vol. 25, pp. 371-393.

**Riccio, A., Marciano, L.** (2005): Effects of Geometrical and Material Features on Damage Onset and Propagation in Single-lap Bolted Composite Joints under Tensile Load: Part I – Experimental Studies, *Int. Journal of Composite Materials*, doi:10.1177/0021998305052026.

**Riccio A.** (2005): Effects of Geometrical and Material Features on Damage Onset and Propagation in Single-lap Bolted Composite Joints under Tensile Load: Part II – Numerical Studies, *Int. Journal of Composite Materials*, doi:10.1177/0021998305052027.

**Sandhu, R. S.** (1974): Nonlinear Behavior of Unidirectional and Angle Ply Laminates, *AIAA Journal of Aircraft*, Vol. 13, pp. 104-111.

**Sleight, D.W.** (1999): Progressive Failure Analysis Methodology for Laminated Composite Structures, NASA/TP-1999-209107.

**Sleight, D.W. KNight, N.F. and Wang, J.T.** (1997): Evaluation of a Progressive Failure Analysis Methodology for Laminated Composite Structures, *AIAA paper*, 97-1187.

**SMR, Inc.** (2005): B2000 MANUALS (release 2.6). Bienne, C.

**Tessler, A., Riggs, R. R.** (1994): Accurate Interlaminar Stress Recovery from Finite Element Analysis, NASA TM-109149.

**Tolson, S., Zabaras, N.** (1991): Finite Element Analysis of Progressive Failure in Laminated Composite Plates, *Computers and Structures*, Vol. 38, No. 3, pp.361-376.

**Tsai, S. W.** (1984): A Survey of Macroscopic Failure Criteria for Composite Materials, *Journal of Reinforced Plastics and Composites*, Vol. 3, pp. 40-63.

**Tsai, S. W., Wu, E. M.** (1971): A General Theory of Strength for Anisotropic Materials, *Journal of Composite Materials*, Vol. 5, pp. 50-80.